Automated manipulation of zebrafish embryos using an electrothermal microgripper

Zhuo Zhang[1] · Yueqing Yu[2] · Peng Song[2] · Yatao Zhang[2] · Dongming Tian[2] · Huipeng Zhang[2] ·
Hongmiao Wei[2] · Mingyu Cui[2] · Guoning Si[3] · Xuping Zhang[4] (ORCID)

Abstract
We present the first report on automated micro-manipulation of zebrafish embryos using an electrothermally-actuated microgripper. A five-bar linkage compliant microgripper, driven by a V-shaped electrothermal micro-actuator, is designed based on topological optimization. The electrothermally-actuated microgripper is fabricated, tested, and then integrated into a robotic micromanipulation system. The semi-automated manipulation of a single zebrafish embryo, as well as a series of comparison experiments, is carried out. Experimental results demonstrate that the microgripper has reliable capability of picking, moving, holding and releasing the zebrafish embryo. Specifically, it performs fairly well in immobilizing and limiting the excessive deformation of the embryo. Finally, based on teaching, the whole process of zebrafish embryo microinjection is programed and performed automatically, thus demonstrating great strengths and performance of the microgripper in zebrafish embryo micro-manipulation.

1 Introduction

The use of zebrafish as an experimental animal model is rapidly gaining popularity in a variety of fields, such as biology research, investigation of human disease, and drug discovery, etc., by providing a long list of advantages and new features (Saleem and Kannan 2018; Adamson et al. 2018). Microinjection of foreign substances, such as DNA, RNA, protein, and drug compound, etc., into one-cell-stage zebrafish embryo using a fine-tipped needle is one of the key techniques for relevant research and development (Samaee et al. 2017; Parng et al. 2002). For example, the one-cell-stage fertilized embryos can be injected with DNA or RNA to permanently modify their genetic makeup in order to generate transgenic or knock-out zebrafish lines (Murphey and Zon 2006; Pitchar et al. 2019). Morpholinos can be injected into the zebrafish embryo to reduce the expression of a gene product (Jonathan et al. 2009). In contrast to the common choice of mice and rats, zebrafish embryos are laid and fertilized externally, which allows them to be easily manipulated in a variety of ways. Furthermore, the transparency of the zebrafish embryo enables image-based screening and assessment of drug effects (Zhang et al. 2011).

Zebrafish embryo microinjection usually includes a series of operations, such as picking, moving, holding, injecting and releasing (Zhao et al. 2019; Kim et al. 2004; Sophia et al. 2014). However, since the zebrafish embryos are small, highly deformable, fragile, sticky, and free to move in water, microinjection is basically relying on manual operations. The manual manipulation requires a great deal of human time and effort, and the successful rate cannot be guaranteed.

The performance of microinjection depends heavily on the choice of handling devices. As shown in Fig. 1a, one of the simplest devices is the open trough where zebrafish embryos are lined and held against one side of the microscope slide placed onto a petri dish (Jonathan et al. 2009; Xie et al. 2010; Huang et al. 2009). With one side being

✉ Xuping Zhang
xuzh@eng.au.dk

1 School of Modern Posts, Xi'an University of Posts and Telecommunications, Xi'an, China

2 College of Mechanical Engineering and Applied Electronics Technology, Beijing University of Technology, Beijing, China

3 School of Medical Instrument and Food Engineering, University of Shanghai for Science and Technology, Shanghai, China

4 Department of Engineering, Aarhus University, Aarhus, Denmark
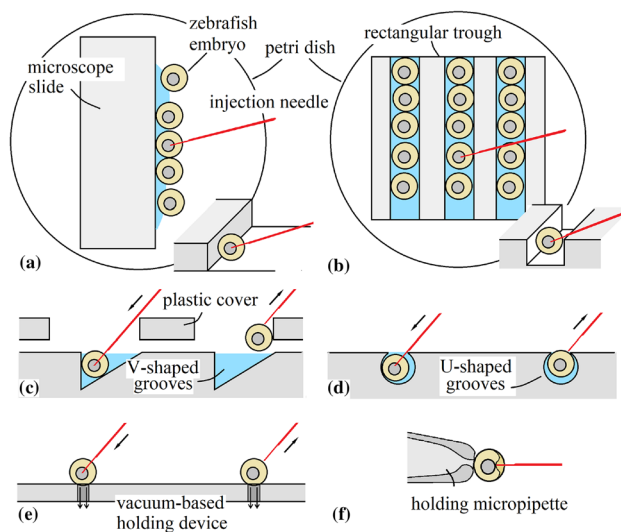
Fig. 1 Handling devices for microinjection of zebrafish embryos: **a** open trough, **b** rectangular trough, **c** V-grooves with a cover, **d** U-grooves, **e** vacuum-based holding device, and **f** holding micropipette

held against the wall, each embryo can therefore be prevented from swimming away while under punctuation. However, it raises the challenge in releasing the embryo as there is no way but using the surface tension of liquid to drag the embryos off from the needle right after injection. In practice, the liquid must be kept at a minimum amount to generate greater surface tension. In addition, the injection micropipette tip has to made be long and thin so that very little resistance occurs when pulling out the needle from the injected embryos. However little liquid immersion may cause the decrease of the embryo survive rate and slender injection micropipette tip tends to be buckled and failed to penetrate the embryo chorion. To tackle this problem, a device with rectangular trough was proposed, as shown in Fig. 1b (Xin and Duan 2018). This device has two sides to limit the movement of the embryo, and releasing the embryos become easier as the right edge of the trough can be used to block the retrieval motion and help get rid of the embryo from the retrieving needle. As shown in Fig. 1c, a V-groove device with an extra cover was further developed to better immobilize and release the embryos (Hogan et al. 2008; Lu et al. 2007). The V-groove can limit the movement of the embryo better since each embryo drops into a groove naturally and is held against the two sides of the groove without a gap. The cover helps the embryo release by pulling the embryos back to the grooves. Note that for both the rectangular trough and V-grooves devices, successful releasing the embryos requires that the injection needle to be kept at a proper angle to make so that the embryos are blocked by the edge when the needle is retrieved. For this reason, researchers (Argenton et al. 2007; Hatta et al. 2006) designed a

U-groove device, as shown in Fig. 1d. The device can be thought of as an improved rectangular trough with a narrower opening. The U-groove makes both embryo immobilization and release much more effective in the manner of hugging the embryos.

However, for all the groove-based devices, the small movement of the embryos cannot be thoroughly prevented since there always exists a gap and room for the embryo to move freely. For this reason, the direction of the injection needle has to be precisely controlled so that the needle is pointed right toward the center of the embryo to prevent the rotation of the cell. These difficulties met in microinjection using the groove-based devices indicate that it is desirable to develop embryo handling devices being capable to actively immobilize the embryos. For this reason, a unique holding device was developed by using the negative air pressure to trap and immobilize the embryos, as shown in Fig. 1e (Wang et al. 2007a, b, 2009). With the negative pressure, the embryos can be firmly immobilized without translation and rotation, and releasing the embryos becomes easy as well. In addition, the negative pressure helps collect and arrange the embryos, and the non-trapped embryos are flushed away from the device. Based on this device, an automated microinjection and batch transferring of zebrafish embryos had been achieved. The shortcoming of this device is that the embryos are not immersed by liquid throughout nearly all the operations from collection, injection, releasing, and transferring. This might cause the decrease of survival rate of the embryos. For this reason, a relatively flexible micropipette was employed to undertake a series of operations including picking, moving, holding and releasing by using the negative pressure (Kim et al. 2004), as shown in Fig. 1f. The micropipette adds enormous flexibilities and adaptivity to nearly all the operations, but at the same time causes difficulties for human to learn how to appropriately use the micropipette. It was proved that both the two types of embryo holding methods experience the difficulty in controlling the local sucking pressure and undertake the risk in damaging the embryos.

In practice, the current handling devices, shown in Fig. 1, are not able to limit the excessive deformations of the embryos in the process of injection as the zebrafish embryos are highly deformable. This causes difficulties for the needle to penetrate the embryos, and even worse the embryos are damaged if the deformation exceeds certain limits. To successfully penetrate the embryo, the needle needs to move at a high instantaneous speed and stop accurately at certain position. This task is apparently among the most difficult manipulations for manual operation. To tackle this problem, several puncturing methods such as pulse-based puncturing (Kimura and Yanagimachi 1995), cutting vibration (Huang et al. 2011), and piezo-electric drill (Johnson et al. 2018), etc. were employed to

assist the needle in puncturing the embryos without causing large deformation. Furthermore, control algorithms were also developed to provide a quick and precise puncturing (Zhou et al. 2010). These methods obviously add the complexity of the system and bring about new problems as well. As a result, nearly all the operations of microinjections relying on current handling devices are performed manually.

Gripping is the most straightforward means for manipulation of micro objects. Up to present, microgrippers driven by various actuation mechanisms have been developed for micro-object manipulations (Verotti et al. 2017; Qu et al. 2016). Among the family of various actuation approaches, such as electro-static (Velosa-Moncada et al. 2018; Gaafar and Zarog 2017), electro-magnetic (Chung et al. 2015; Despa et al. 2014), and piezoelectric (Ruiz and Sigmund 2018; Chen et al. 2017), etc., electrothermal actuation that works on the principle of Joule heating and thermal expansion of beam structures, has been demonstrated to be compact, stable, easy-to-control, large displacement and force actuation techniques (Voicu 2016; Soma et al. 2017). Manipulation of small objects, such as micro blood vessel specimen, micro cell and small Styrofoam ball etc., has been accomplished successfully with electrothermal microgrippers (Chu et al. 2011; Zhang et al. 2010).

Therefore, this work makes the first attempts to develop and use an electrothermally-actuated microgripper for the automated manipulation of the zebrafish embryos. The remainder of the work is organized into the following parts: Sect. 2 describes the design and fabrication of the microgripper. Then, the performance of the microgripper is tested in Sect. 3 based on a micro-robotic system. In Sect. 3, semi-automated micromanipulation experiments of zebrafish embryos as well as comparison experiments are conducted to demonstrate the effectiveness and versatility of the microgripper, and particularly its virtue of immobilizing the embryo and ability of limiting the excessive deformation. In Sect. 4, the fully automated microinjection of zebrafish embryo is performed based on a teaching strategy. In the last section, we conclude with summarization, discussion, and our ongoing research efforts.

2 Structural design and fabrication of an electrothermally-actuated microgripper

2.1 Design of the electrothermal micro-actuator

An electrothermal micro-actuator generates a displacement and force due to the thermal expansion of its beam structure. Various types of beam structures have been proposed

in order to make the generated displacements and forces as large as possible. Among them, the V-, Z- and U-shaped beams (Zhang et al. 2017a, b, c, 2018a, b, c) emerged as the basic beam types for constructing more complex actuators. The U-shaped beam offers arc circular motion due to the difference of thermal expansions of a pair of thin and thick beams. Compared with V- and Z-shaped beams, the U-shaped beam generates much smaller displacement and force and undergoes an overshoot in reaching the steady state (Zhang et al. 2017b). The V- and Z-shaped actuators, on the other hand, produce rectilinear motion thanks to their symmetric structures. In practice, the rectilinear motion is preferred for developing more complex systems by combining the V- or Z-shaped actuators with compliant mechanisms. Since V- or Z-shaped beams are not required to overcome each other to generate a motion, there is no overshoot and much larger displacement and force can be generated (Zhang et al. 2017a, b, c). Although the V- and Z-shaped actuators share many characteristics in common, the V-shaped actuator offers much larger force (Zhang et al. 2018a).

Therefore, the V-shaped actuator is chosen to drive the gripper mechanism for producing the larger displacement of the gripper jaws. The schematic diagram of a V-shaped actuator is shown in Fig. 2. The working principle of the V-shaped electrothermal actuator is simple. When applying a voltage on the two end pads of the actuator, the whole beam is heated and elongated due to the thermal expansion. As a result, the middle shuttle will be pushed forward thus producing a displacement and force.

In the authors' previous work, an analytical model of the V-shaped electrothermal actuator was established as

$$y_{max} = \begin{pmatrix} F_1 & -F_2 \end{pmatrix} \begin{pmatrix} U^2 \\ P \end{pmatrix} \qquad (1)$$

where y_{max} is the output displacement. U and P are the input voltage and external force respectively. $F_1 = \alpha Q B_1 T$, $F_2 = B_2/(2nE)$, F_1 and F_2 refer to the flexibility of the actuator in reaction to the voltage and external force
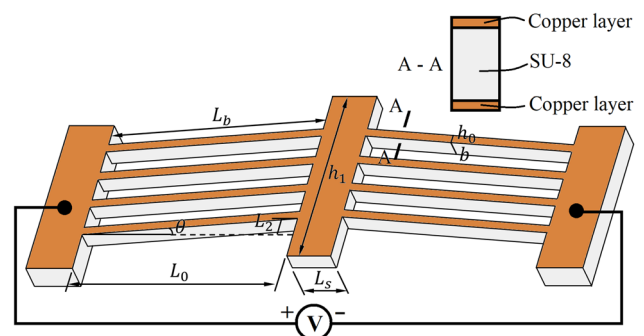

Fig. 2 Schematic diagram of a V-shaped electrothermal micro-actuator

respectively. α, Q, and E are its material properties. B_1 and T are its structural parameters. n is the number of pairs of beams.

The analytical model was validated through both simulation and experimental testing. Detailed results and discussion can be found in (Zhang et al. 2015a, b, 2017c). Based on the analytical model, comprehensive parameter analyses are conducted, and it is found that, the output displacement of the V-shaped actuator depends heavily on the parameters of L_2 and L_0. As illustrated in Figs. 3 and 4, the V-shaped beam with small L_2 and large L_0 can produce the largest displacement (Zhang et al. 2015a).

In our published conference paper (Zhang et al. 2018a), a V-shaped actuator with four pairs of beams were fabricated and tested. The dimensions are listed in Table 1. The actuator was made of SU-8 photoresist with very thin copper layers being deposited on both two surfaces of the structure. The copper layers are conductive and are heated first when applying a voltage. Then the beam structure is heated and elongated. Apparently, a thicker beam results in greater stiffness of the structure, and a larger force is required to push the shuttle forward. The initial design of a V-shaped actuator in (Zhang et al. 2018a) can produce a maximum displacement of only 10 μm under a voltage of 0.5 V, as listed in Table 2. However, 10 μm is far from enough to grip a zebrafish embryo with the diameter of around 600 μm $\sim$ 800 μm. Based on the parameter analyses, a modified and improved V-shaped actuator, with dimensions listed in Table 1, is designed in this work. The improved V-shaped actuator can offer a maximum displacement of 65.59 μm under a voltage of 0.5 V, as listed in Table 2.

2.2 Topology optimization of the microgripper mechanism

The role of the gripper mechanism is to convert the input displacement to gripping motion and force. In this work, the gripper mechanism is designed using topology optimization. The design domain with several constraints is shown in Fig. 5a, in which $F_{actuator}$ is the input force of the
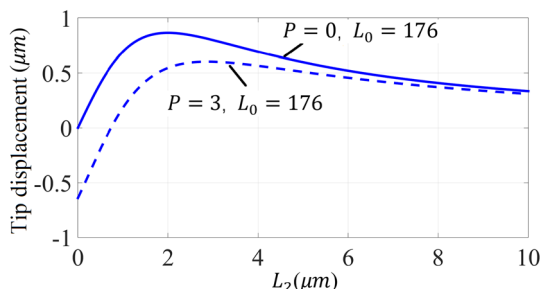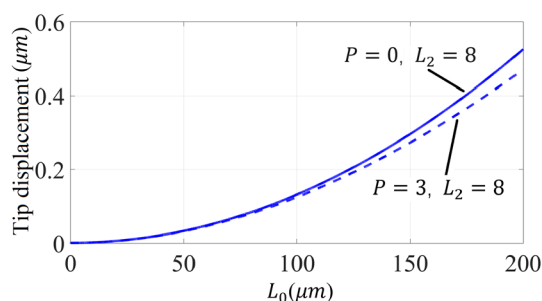

Fig. 3 Tip displacement vs. L_2

Fig. 4 Tip displacement vs. L_0

Table 1 Dimensions of the V-shaped actuator (unit of length: μm)

	b	h_1	L_s	h_0	L_2	L_0
Initial	230	2459.7	262.9	68.3	140.7	1333.5
Improved	180	3592.3	473.4	139.3	313.6	3635.8

Table 2 Output displacement of the V-shaped actuator (unit of length: μm)

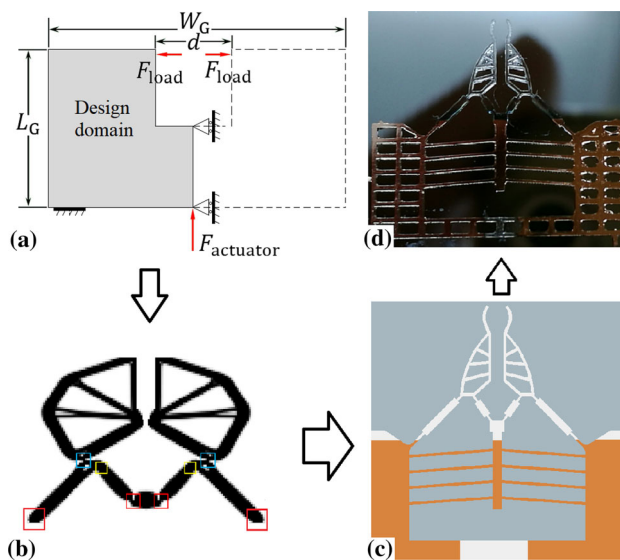| Voltages (V)	0.1	0.2	0.3	0.4	0.5
Displacement					
Initial	0	2.03	4.07	7.12	10.17
Improved	3.39	11.42	22.00	40.62	65.59

Fig. 5 Topology optimization and fabrication of the microgripper mechanism: **a** design domain and boundary conditions, **b** initial topology structure, **c** optimized electrothermally-actuated microgripper structure, and **d** fabricated electrothermally-actuated microgripper

V-shaped actuator and F_{load} refers to the gripping force on the gripper jaws. As topology optimization has become a

matured method in designing structures, the designing detail steps and calculations are not be presented in this work. The optimization problem is formulated as

$$\text{Find} \quad x = (x_1, x_2, \ldots, x_n)^T$$

$$\text{Min} \quad C(x) = F^T U$$

$$\text{S.T.} \quad \begin{cases} V \leq V^* \\ F = KU \\ 0 < x_{min} \leq x_i \leq 1 (i = 1, 2, 3, \ldots n) \end{cases} \quad (2)$$

in which x_i represents the relative density of one element. In this work, the continuum approach is used, and the design domain has been meshed into many small elements. The value of the relative density of one element is 0 or 1. 0 and 1 represent void and solid element, respectively. $C(x)$ is the structural flexibility. U is the displacement vector. F is the structural force vector. V and V^* refer to the volume after and before optimization respectively. Usually, the value of design variable x_i cannot be smaller than 0.01 to avoid the singularity of the stiffness matrix.

By solving this optimization problem, the topology layout of a gripper mechanism is derived, as shown in Fig. 5b. By replacing the narrow areas highlighted by rectangles with compliant hinges, a five-bar linkage compliant gripper can be obtained as shown in Fig. 5c. The jaws of the gripper are designed to be featured with arc circular geometry in order to effectively hug and confine the deformation of the zebrafish embryos. When a voltage is applied on the two pads of the V-shaped actuator, the shuttle will be pushed forward due to thermal expansion of beams. The motion will then be transferred to the gripper jaws via the gripper mechanism. Apparently, in order to generate gripping motion, the V-shaped actuator should be able to produce a large force.

2.3 Fabrication of the microgripper

Fabrication of the electrothermally-actuated microgripper is based on MEMS (Micro-Electronic-Mechanical-System) micromachining process, which consists of two main steps: fabrication of the whole structure (V-shaped actuator and gripper) using SU-8 photoresist, and deposition of the copper layer on the two surfaces of the actuator area. The microgripper made of SU-8 photoresist is biocompatible and can generate large displacement under low voltages with large thermal expansion and small Young's modulus. The fabricated electrothermally-actuated microgripper is shown in Fig. 5d.

As illustrated in Fig. 6, detailed fabrication process is divided into seven steps:

(a) Prepare a silicon substrate with a 2 μm thick sacrificial layer of silicon dioxide.
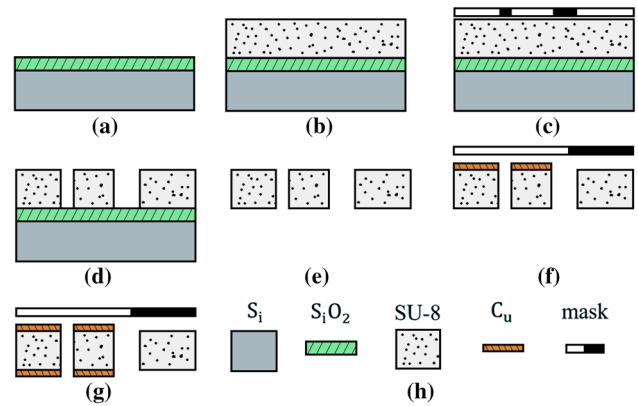

Fig. 6 Fabrication process of the microgripper. **a** Prepare the substrate **b** spread SU-8 photoresist and pre-bake **c** exposure and post-bake **d** pattern and hard-bake **e** release and levelling **f** deposit on the positive surface **g** deposit on the negative surface **h** legends

(b) Spin a layer of SU-8 2150 photoresist to uniformly spread it on the surface of the substrate at a speed of 500 rpm for 10 s. Then, Pre-baking is conducted at 65 °C for 30 min and 95 °C for 110 min.

(c) Conduct exposure using a BGJ-3B lithography system for 15 min., and post exposure bake at 65 °C for 10 min and 90 °C for 30 min.

(d) Pattern the SU-8 and perform hard bake at 150 °C for 15 min.

(e) Release sacrificial layer of silicon dioxide and level the SU-8 structure layer. Now the whole structure, including actuator and gripper mechanism, was fabricated.

(f) Deposit a chrome layer on the surface of the SU-8 layer. Copper is then deposited on the chrome surface using a JS3X-100 deposition system for 10 min.

(g) Conduct the deposition of the other surface of SU-8 as in (f). For both steps (f) and (g), mask is used to prevent deposition on the gripper mechanism area.

3 Experimental setup and testing

3.1 Experimental setup

A robotic micromanipulation system is established as shown in Fig. 7a. The robotic system consists mainly of an inverted microscope, a CCD camera, a precision stage with X- and Y-axes translational motion freedom and one Z-axis focusing motion, a pair of micromanipulators with three axes translational motion freedoms (CFT8301D2, with the travel range of 26 mm for each axes, each pulse equals to 0.047 μm), power supply, and a computer. The fabricated microgripper is mounted on a PCB board and to the left
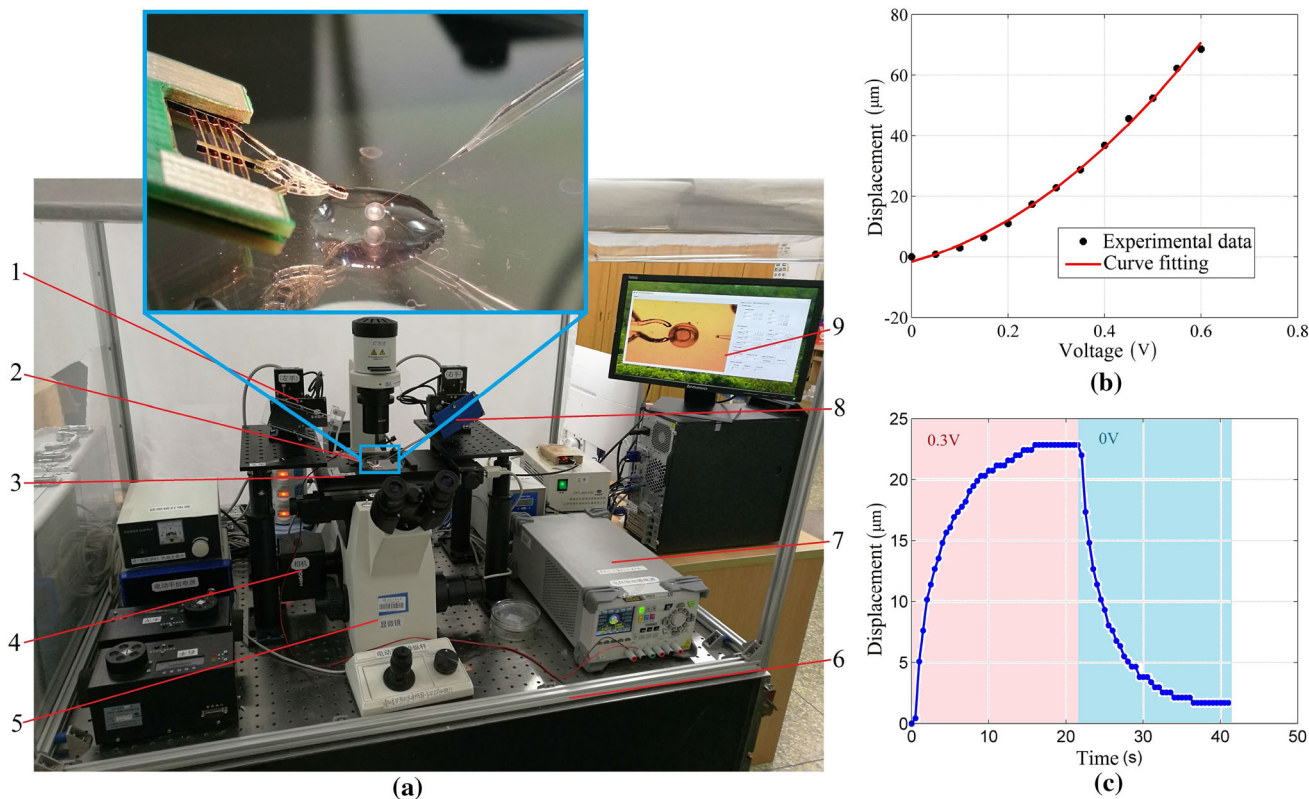
Fig. 7 A robotic micromanipulation system and performance testing of the microgripper: **a** Robotic micromanipulation system: 1. Micromanipulator, 2. Electrothermally-actuated microgripper, 3. Precision Stage, 4. CCD Camera, 5. Microscope, 6. Anti-vibration Table, 7. Power Supply, 8. Micromanipulator, and 9. Computer and software interface, **b** displacements vs. voltages, **c** displacement vs. time

manipulator. An injection micropipette is mounted on the right manipulator. The zebrafish embryos are collected on the petri dish which is loaded on the precision stage. The role of the precision stage is to move the zebrafish embryos into the field of view and the focus of the camera. All the components of the robotic system are integrated into an in-house developed software to achieve more reliable, quicker, and greater repeatability compared to manual operation by using joy sticks.

3.2 Static and dynamic performance testing of the electrothermally-actuated microgripper

The steady-state tip displacements of one side of the gripper jaws are measured under different input voltages, as shown in Fig. 7b. It is seen that the tip of the gripper jaw can generate a displacement of around 70 μm under a voltage of 0.6 V. For the size of the zebrafish embryo, the displacement of 70 μm at one side of the gripper is satisfactory. The dynamic response of the gripper is also tested under voltages of 0.3 V, as shown in Fig. 7c. It is seen that when applied a voltage, the jaws open and reach the

steady-state position smoothly, without an overshoot. When the voltage drops to zero, the gripper jaws returns to the initial position following the same dynamic curve. The smooth evolution of the displacement is important for zebrafish embryo micromanipulations. First, quick jaws open and close at the beginning will increase the effectiveness of the embryo release and the efficiency of the overall manipulations. Second, for gripping, slowly close the gripper jaws offers the gentle and compliant hugging to the zebrafish embryo. Last but not least, the gripper jaws reach the steady state without an overshoot. This is important for the effective and safe gripping of embryos.

The output displacements of the electrothermal actuator and the microgripper are measured based on this robotic system via image matching. In this work, least square error method is used to realize image matching. First, a local square image with obvious features is captured as the template for matching. Second, search every column and row throughout the source image, and calculate the square errors of pixel values between every points in the source image $T(x', y')$ and the corresponding points in the template image $I(x + x', y + y')$. Then, for every searching point, a square error R_{sq_diff} can be derived as

$$R_{sq\_diff} = \sum_{x',y'} [T(x',y') - I(x+x', y+y')]^2 \qquad (3)$$

Clearly, most matching point will be the position with least square error. Based on image matching, the position of the template for every time instant can be obtained. Then, the output displacement is derived. Figure 8a, b show the image matching for the gripper and the actuator, respectively.

However, when applied a voltage of 0.55 V for the first time, a sudden drop of the displacement occurs in reaching the steady state. After the voltage is off, the gripper jaws return to zero and proceed to the negative direction, as shown in Fig. 9. This phenomenon could be explained by: (1) under a high voltage, a larger expansion of V-shaped beams is created, (2) if the stiffness of the gripper mechanism is large, the axial force can be accumulated to exceed certain limits and buckled. The buckling causes the V-shaped beams to jump to another more stable position. Obviously, the buckling leads to the plastic deformations of the V-shaped beams, since for the second time, when applied the same voltage of 0.55 V, the buckling no longer occurs. This phenomenon could be explained by that the SU-8 photoresist can be easily soften when heated, and the buckling takes place to and causes the V-shaped beam to generate plastic deformation, and then to release energy and jump down to a more stable state. For a higher voltage of 0.6 V, the similar phenomenon is observed.

3.3 Semi-automated micromanipulation of a zebrafish embryo

Before we try to implement a fully automated manipulation of zebrafish embryos, in this section an experiment of semi-automated manipulation of zebrafish embryo is conducted, as shown in Fig. 10. "Semi-automated" means the manipulation is carried out by moving every step by specifying the step length values or voltages into the robotic system software, instead of manually operate the joy sticks. First, a zebrafish embryo is collected and transferred into petri dish, and place the petri dish on the precision stage. Second, the injection micropipette is prepared and the front tip is cut to ensure the diameter of the
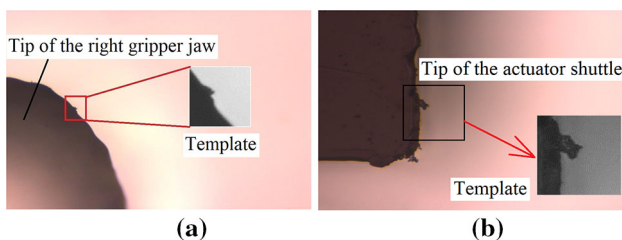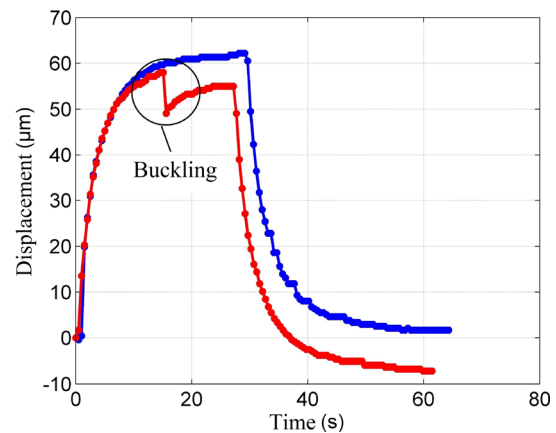

Fig. 9 Buckling of the microgripper (displacement vs. time, under 0.55 V): red line represents first time applying the voltage; blue curve is the second time applying the voltage

tip to be around 10 μm. To prevent possible buckling, the needle diameter cannot be too small.

Detailed steps of the micro-manipulation include: (a) Move the embryo to the field of view with precision stage. Then move the jaws of microgripper to just over the embryo, and the injection needle to the field of view. The tip of the needle should be positioned in the middle of FOV (field of view). (b) Open the jaws of the microgripper by applying a voltage of 0.8 V and move the gripper down into the water. (c) Specify the input voltage to zero to close the jaws and grip the embryo. Then, move the gripper jaws to the center of view to position the embryo to the center of FOV. (d) Move the injection needle until the tip touches the chorion. (e) Continue to penetrate the embryo until the needle tip reaches the maximum depth where the tip is about to penetrate the chorion. (f) Let the needle penetrate the embryo and enter the perivitelline. (g) Continue to penetrate the yolk. (h) Move the injection needle back to the original position and complete the whole penetration. Finally, open the jaws and release the embryo.

It is seen from Fig. 10 that the jaws of the gripper form a geometric confine to hug and firmly grip the embryo. In positioning the embryo, there is nearly impossible for the embryo to drop off. Particularly, the excessive deformation of the embryo under penetration is limited. This facilitates the penetration process, and extra punctuation methods as well as control algorithms are no longer required, releasing the embryo also becomes relatively easy by simply pulling the needle out.

3.4 Comparison experiments

In order to further demonstrate the advantages of the developed microgripper in this work, two more groups of comparison experiments are conducted. In Group 1, each

Fig. 8 Templates for image matching: **a** actuator and **b** microgripper
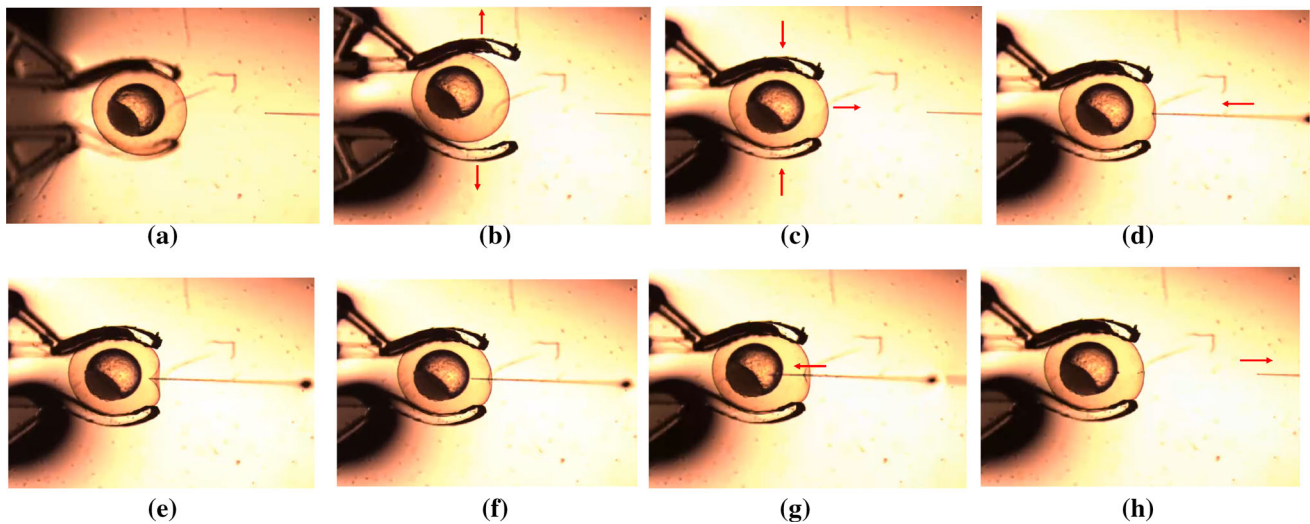
Fig. 10 Micromanipulation of a one-cell zebrafish embryo: **a** gripper jaws above the embryo, **b** gripper jaws into water and open to grip the embryo, **c** gripper jaws close, gripped and move the embryo to the center of view, **d** tip of micropipette touches the chorion, **e** the moment at which the tip of the injection micropipette is about to penetrate the chorion, **f** micropipette into the perivitelline, **g** micropipette into the yolk, and **h** micropipette withdraw

embryo is penetrated with only its one side against the microscope slide wall, as shown in Fig. 11a, b and f. In Group 2, each embryo penetration is performed with its two sides against the microscope slide wall, as shown in Fig. 11c–e, g and h. The role of the wall is to limit the movement of the embryos under penetration. Since the embryos are immersed and float in the water, to penetrate the embryo successfully, the needle tip should be right directed to the center of the yolk otherwise the embryo may rotate, as shown in Fig. 11a–d. Figure 11a and c illustrates

the initial position where the embryo is ready to be penetrated. It is much different from the scenario in which the gripper jaws hug the embryo firmly as shown in Fig. 10, the microscope slide wall only limits the movement of the embryo in certain directions, and the embryo is still free to rotate and move towards other directions. This causes difficulties in releasing the embryo as shown in Fig. 11e.

In addition, the experiments demonstrate that the wall does not help limit the deformation of the embryo while being penetrated. The unwanted consequence is as shown
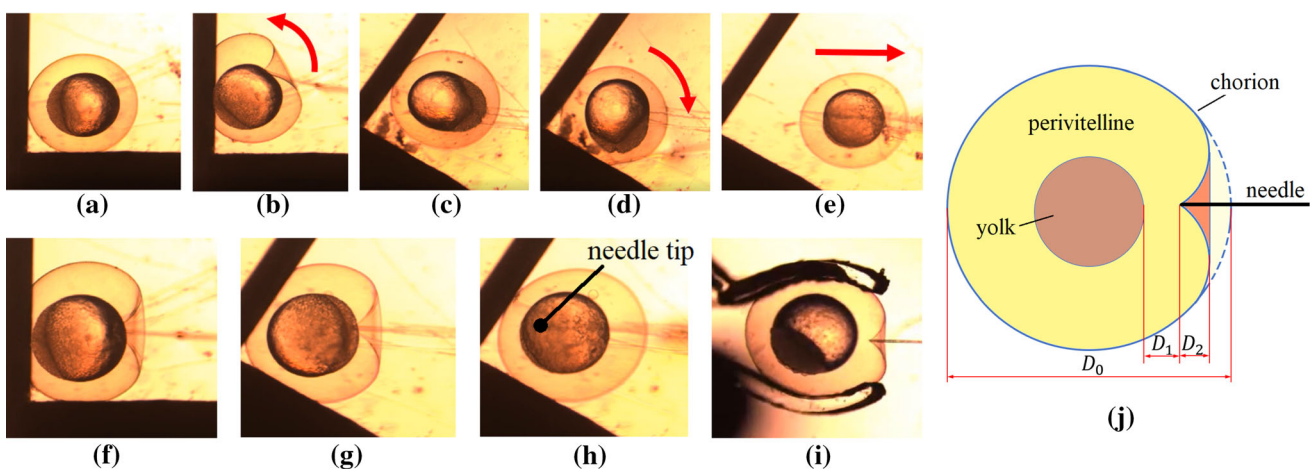
Fig. 11 Penetration of zebrafish embryos: **a** the embryo ready to be penetrated (Group 1), **b** needle failed to penetrate the embryo causing the embryo rolling (Group 1), **c** the embryo ready to be penetrated (Group 2), **d** needle failed to penetrate the embryo causing the embryo rolling (Group 2), **e** needle fail to release the embryo after penetration, **f** the moment the needle tip is about to penetrate (Group 1), **g** the moment the needle tip is about to penetrate (Group 2), **h** needle tip into the yolk of the embryo, **i** the moment the needle tip is about to penetrate (using the microgripper), and **j** illustrative diagram of evaluation of embryo deformations

in Fig. 11f and g. Due to the large deformation, the needle tip reaches to the yolk of the embryo but still not be able to puncture the chorion. To evaluate and compare the deformation of the embryos under penetration, a set of parameters are used, as illustrated in Fig. 11j, in which D_0 is the diameter of the embryo, D_1 is the distance between the yolk and the needle tip at the moment when the needle is about to penetrate the embryo, and D_2 is the maximum depth that the needle can reach before the tip is about to puncture the chorion. The relative parameters, i.e., $d_1(= D_1/D_0)$ and $d_2(= D_2/D_0)$ are defined and used to eliminate the effect of the diameter of the embryos.

As shown in Table 3, the microgripper can significantly limit the deformation of the zebrafish embryo since the maximum depth that the tip needs to reach to puncture the chorion is only 10.19%. In contrast, 21.53% deformation occurs for Group 1 with the one side of the zebrafish embryo against a wall, while little smaller, still up to 19.28% maximum deformation for Group 2 with two sides against walls.

Furthermore, it can be seen in Table 3, the value of d_1 for Group 1 and 2 is both negative. This means for both Group 1 and 2: (1) the tip of the needle reaches inside the yolk while still not being able to pierce the chorion of the embryos, as shown in Fig. 11f and g; (2) the needle penetrated directly to the yolk deeply without reaching the perivitelline space first. Apparently, this is not suited to the applications in which the injection materials are required to be only injected into the perivitelline space (Ren et al. 2017), and even worse it can damage the embryo if deformation exceeds certain limits. In contrast, in the case of the injection with the developed microgripper, the value of d_1 is positive, which means the tip of the needle can reach into the perivitelline space first then to the yolk. In comparison, Group 2 performs better than Group 1 in limiting the deformation of the embryo since the deformation is prevented along more directions. Similarly, other devices shown in Fig. 1 have no means to limit the deformation of the embryo as well. For the gripper, the jaws almost limit the deformation of the embryo in nearly all directions.

**Table 3** Deformation evaluation of zebrafish embryo (unit of length: µm)

	D_1	$d_1(\%)$	D_2	$d_2(\%)$	D_0
Microgripper	64	8.58	76	10.19	746
One side against the wall	− 67	− 9.02	160	21.53	743
Two sides against the walls	− 32	− 4.26	145	19.28	752

4 Automated micro-manipulation of a zebrafish embryo

The semi-automated micromanipulation experiments of a zebrafish embryo have demonstrated that the effectiveness and reliability of the developed electrothermally-actuated microgripper for picking, holding, and releasing the zebrafish embryos. In this section, fully automated manipulation of the zebrafish embryos is performed using the developed microgripper. Specifically, the fully automated manipulation is implemented with a teaching strategy, all the steps and values are pre-specified and integrated into the system software before clicking the start button.

Based on the experiments of the semi-automated manipulations, the gripper jaws are better to be placed at the height of around 700 µm to the bottom of the petri dish. As the height of the microgripper cannot be measured, we adopt a very simple method to estimate the position of the gripper. First, move the gripper in the z-axis, i.e., perpendicular to the petri dish plane, until the gripper jaws create a displacement in the plane, which indicates the gripper jaws have hit the bottom of the petri dish. Then, lift the gripper up to the position of 700 µm and continue moving 70.5 µm (i.e., 1500 pulses) to get out of the water. Now by specify the values of each steps, the manipulation can perform automatically.

In order to completely test the performance of the microgripper and the robotic system, a much more complex manipulation procedure is designed for the testing. Figure 12 shows the complete steps and procedure of the zebrafish embryo micro-manipulation. First, move the gripper and the embryo to center of the view, as shown in step (a). This is determined to be the best position for gripping and monitoring the embryo, i.e., the gripper only needs to open the jaws, down to the water, and then close the jaws a little to grip the embryo. If the gripper immersed into the water first, then approach the embryo, the embryo will be very likely to swim away. In step (a), the needle also is to be placed in parallel to the gripper and pointed towards the center of the embryo. In step (b), move the gripper, embryo and the needle back to initial positions and record the number of pulses for each step. The gripper first moves to negative direction along X axis with 800 pulses, and then to the positive direction along Y axis with 2000 pulses. The needle moves to positive direction along Y axis with 1000 pulses. Then, the precision stage moves to negative direction of Y axis and positive direction of X axis with 5000 pulses to place the embryo to initial position. Now, the gripper, needle and the embryo are at initial position and the manipulation is ready to start. Step (c) and (d) are the inverse of the step (b), i.e., move the embryo, gripper, and the needle to the gripping position as in step
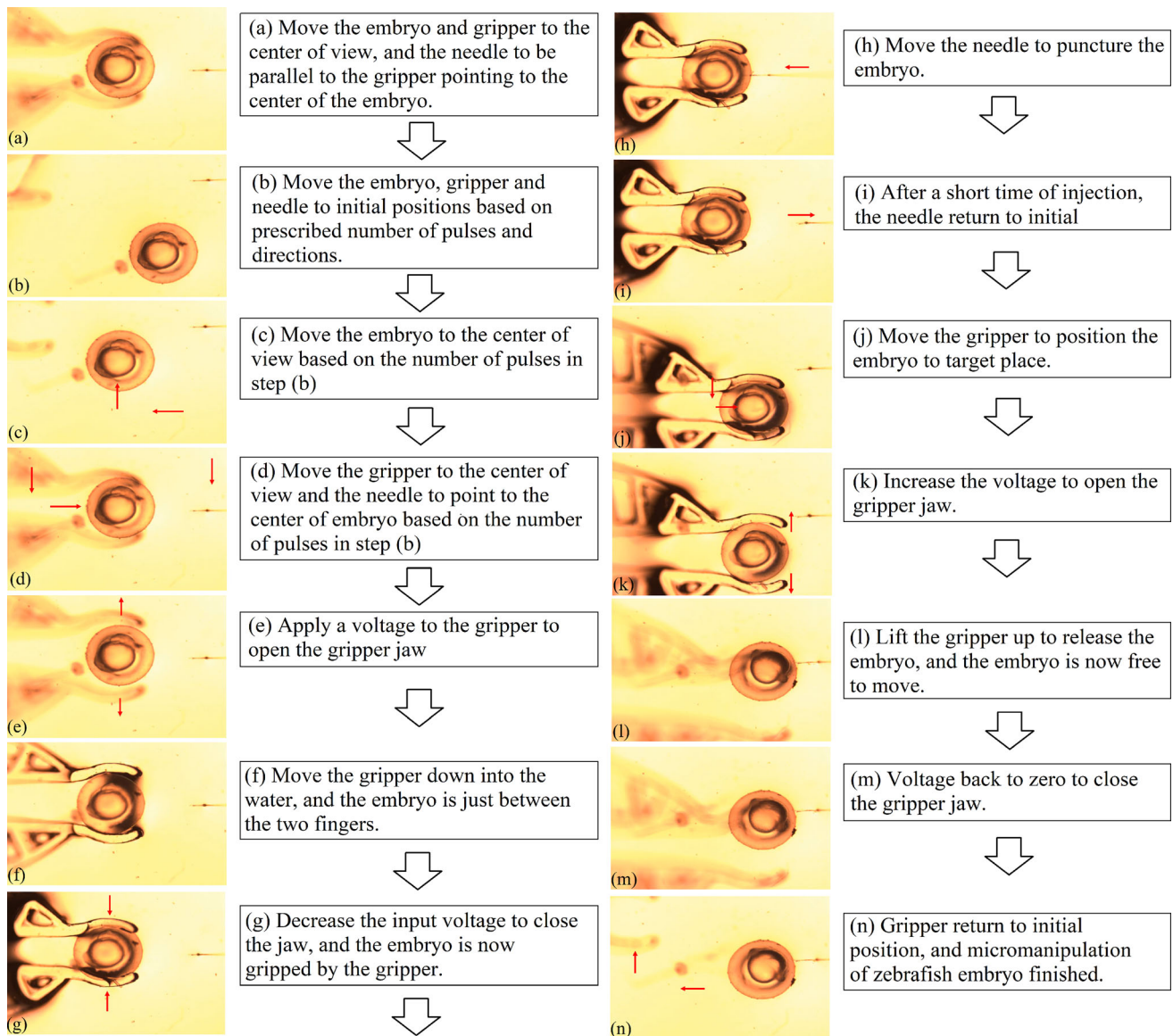
Fig. 12 Automated micro-manipulation of the zebrafish embryo

(a) based on the pulses specified in step (b). Note that, from step (c) on, all the pulses, voltages and duration time, etc., are specified beforehand. Simply clicking the start button in the software, the micromanipulation of the embryo will be conducted automatically following the prescribed steps and values. Clearly, the automated manipulation is open loop and the performance enormously depends on the effectiveness and reliability of the gripper.

According to the testing under 0.6 V, each jaws of the gripper can produce the displacement of around 70 μm. Higher voltages may cause oxidation and even failure of the actuator. In step (e), apply a voltage of 0.6 V to open the jaws, followed by step (f), moving the gripper down with 1500 pulses, i.e., 70.5 μm, to position the gripper jaws at the same level of the embryo. Now the embryo is right in

between the gripper jaws. In step (g), decrease the voltage to 0.4 V (or 0.1 V) to close the jaws slightly. The embryo is then firmly gripped by the gripper. In order to avoid causing any damage to the embryo, the voltage should not set to zero to close the jaws completely.

In step (h), move the needle to negative direction of X axis with 1500 pulses to puncture the embryo. To simulate injection process, leave the needle there for 3 s until the injection is finished. After injection, in step (i), move the needle to the positive direction of X axis with 1500 pulses to return the needle. To simulate the alignment of the embryos after injection, in step (j), move the gripper to the positive direction of X axis and the negative direction of Y axis with 1000 pulses respectively. Then, in step (k), increase voltage to release the embryo. In step (l), lift the

Table 4 Summary of automated micro-manipulation of zebrafish embryos

Groups	Total time (s)	Injection time (s)	Switch time (s)	Jaws open/close time (s)	Jaws close voltage (V)
A	54	3	1.5	6	0.4
B	40	3	1.0	6	0.4
C	37	3	0.8	5	0.1

gripper up with 1500 pulses, i.e., 70.5 μm, to get gripper jaws out of water, and the embryo is released completely. In step (m), the voltage returns to zero to close the gripper jaws. In the final step, move the gripper to the negative direction of X axis and the positive direction of Y axis with 3000 and 1800 pulses respectively to return the gripper to the initial position. At this point, the micro-manipulation of zebrafish embryos is finished. Note that, between any two steps, a short switch time is specified as shown in Table 4. We also leave enough time for the gripper jaws to open and close, as listed in Table 4. Three groups of experiments are conducted, as summarized in Table 4. By reducing the switch time and jaws open/close time, the single manipulation experiment takes only 37 s. The manipulation time can be even shorter by reducing the injection, switch, and jaws open/close time, and further simplifying the whole procedure.

5 Conclusion

In this work, we have achieved automated manipulation of zebrafish embryos using a microgripper driven by a V-shaped electrothermal actuator. First, the V-shaped actuator is designed based on parameter analyses. Second, a symmetric five-bar linkage gripper mechanism is proposed with topology optimization. Then, the electrothermally-actuated microgripper is fabricated via MEMS micro-machining process and integrated into a micro-robotic manipulation system. Both the static and dynamic performances have been tested on the robotic system. Semi-automated manipulation of the zebrafish embryo has been accomplished successfully using the gripper. Experimental testing has demonstrated that the micro-gripper can well pick, hold, move, and release the embryos without causing any damage to the cells. Particularly, the gripper jaws can firmly hug the embryo thus nearly completely limiting the excessive deformation of the embryo under punctuation. Finally, several groups of experiments with teaching-based automated zebrafish embryo manipulation have been achieved. The experiments have further demonstrated the great effectiveness and reliability of the microgripper for zebrafish embryo manipulation.

Our ongoing work focuses on (1) the intelligent and automated micro-manipulation of zebrafish embryos. In doing this, image recognition algorithms will be utilized to reduce and even replace human interventions. (2) Quantification and evaluation on the actuation speed, actuation precision and the safety of the microgripper by adding force measurement devices and running large amount of experiments for practical and specific applications.

References

Adamson KI, Sheridan E, Grierson AJ (2018) Use of zebrafish models to investigate rare human disease. J Med Genet 55:641–649

Argenton F, Bitzur S, Yarden A (2007) An inexpensive and easy microinjection embryo-tray. Zebrafish book 5th edition

Chen T, Wang Y, Yang Z, Liu H, Liu J, Sun L (2017) A PZT actuated triple-finger gripper for multi-target micromanipulation. Micromachines 8(2):33

Chu J, Zhang R, Chen Z (2011) A novel SU-8 electrothermal microgripper based on the type synthesis of the kinematic chain method and the stiffness matrix method. J Micromech Microeng 21(5):054030

Chung SE, Dong X, Sitti M (2015) Three-dimensional heterogeneous assembly of coded microgels using an untethered mobile microgripper. Lap Chip 15(7):1667–1676

Despa V, Catangiu A, Ivan IA, Gurgu V, Ardeleanu M (2014) Modeling and control of a microgripper based on electromagnetic actuation. Sci Bull Valahia Univ Mater Mech 9:131–136

Gaafar E, Zarog M (2017) A low-stress and low temperature gradient microgripper for biomedical applications. Microsyst Technol 23(12):5415–5422

Hatta K, Tsujii H, Omura T (2006) Cell tracking using a photoconvertible fluorescent protein. Nat Protoc 1(2):960–967

Hogan BM, Verkade H, Lieschke GJ, Health JK (2008) Manipulation of gene expression during zebrafish embryonic development using transient approaches. Methods Mol Biol 469:273–300

Huang H, Sun D, Mills JK, Li J, Cheng SH (2009) Visual-based impedance control of out-of-plane cell injection systems. IEEE Trans Autom Sci Eng 6:565–571

Huang H, Mills JK, Sun D (2011) A universal piezo-driven ultrasonic cell microinjection system. Biomed Microdevices 13:743–752

Johnson W, Dai C, Liu J, Wang X, Luu DK, Zhang Z, Ru C, Zhou C, Tan M, Pu H (2018) A flexure-guided piezo drill for penetrating the zona pellucida of mammalian oocytes. IEEE Tran Biomed Eng 65:678–686

Jonathan NR, Michael FS, John DM (2009) Microinjection of zebrafish embryos to analyze gene function. J Vis Exp 25:1115

Kim DH, Sun Y, Yun S, Kim B, Hwang CN, Nelson B, Lee SH (2004) Mechanical property characterization of the zebrafish embryo chorion. Conf Proc IEEE Eng Med Biol Soc 7:5061–5064

Kimura Y, Yanagimachi R (1995) Intracytoplasmic sperm injection in the mouse. Biol Reprod 52:709–720

Lu Z, Chen P, Nam J, Ge R, Lin W (2007) A micromanipulation system with dynamic force-feedback for automatic batch microinjection. J Micromech Microeng 17(2):314–321

Murphey RD, Zon LI (2006) Small molecule screening in the zebrafish. Methods 39(3):255–261

Parng C, Seng WL, Semino C, McGrath P (2002) Zebrafish: a preclinical model for drug screening. Assay Drug Dev Technol 1(1 Pt 1):41–48

Pitchar A, Rajaretinam RK, Freeman JL (2019) Zebrafish as an emerging model for bioassay-guided natural product drug discovery for neurological disorders. Medicines (Basel) 6(2): 6020061(20 pp)

Qu J, Zhang W, Jung A, Silva-Da CS, Liu X (2016) Microscale compression and shear testing of soft material using an MEMS microgripper with two-axis actuators and force sensors. IEEE Trans Autom Sci Eng 14(2):834–843

Ren J, Liu S, Cui C, Ten D (2017) Invasive behavior of breast cancer cells in embryonic zebrafish. J Vis Exp 122:e55459 (9 pp)

Ruiz D, Sigmund O (2018) Optimal design of robust piezoelectric microgrippers undergoing large displacements. Struct Multidiscip Optim 57(1):71–82

Saleem S, Kannan RR (2018) Zebrafish: an emerging real-time model system to study Alzheimer's disease and neurospecific drug discovery. Cell Death Discov 4:45

Samaee SM, Nikkhah H, Varga ZM, Rezaei B (2017) A simple and inexpensive microinjection system for zebrafish embryos and larvae. Zebrafish 14(6):581–585

Soma A, Iamoni S, Voicu R, Muller R (2017) Design and experimental testing of an electro-thermal microgripper for cell manipulation. Microsyst Technol 24(1):1–8

Sophia S, Nadia K, Reinhold H, Ulrike K (2014) Microinjection into zebrafish embryos (Danio rerio). Environ Sci Eur 26(1):1–8

Velosa-Moncada L, Aguilera-Cortes L, Gonzalez-Palacios M, Raskin JP, Herrera-May AL (2018) Design of a novel MEMS microgripper with rotary electrostatic comb-drive actuators for biomedical applications. Microsyst Technol 18(5):1664

Verotti M, Dochshanov A, Belfiore N P (2017) A comprehensive survey on microgrippers design: mechanical structure. J Mech Des 139(6):060801 (26 pp)

Voicu RC (2016) Design, numerical simulation and experimental investigation of an SU-8 microgripper based on the cascaded V-shaped electrothermal actuators. J Phys Conf Ser 757(1):012015

Wang W, Liu X, Sun Y (2007) Autonomous zebrafish embryo injection using a microrobotic system. In: 2007 IEEE international conference on automation science and engineering, AZ USA, September 22–25

Wang W, Liu X, Gelinas D, Ciruna B, Sun Y (2007b) A fully automated robotic system for microinjection of zebrafish embryos. PLoS One 2(9):e862

Wang W, Liu X, Sun Y (2009) High-throughput automated injection of individual biological cells. IEEE Trans Autom Sci Eng 6(2):209–219

Xie Y, Sun D, Liu C, Tse HY, Cheng SH (2010) A force control approach to a robot-assisted cell microinjection system. Int J Robot Res 29(9):1222–1232

Xin Y, Duan C (2018) Microinjection of antisense porpholinos, CRISPR/Cas9 RNP, and RNA/DNA into zebrafish embryos. Methods Mol Biol 1742:205–211

Zhang R, Chu J, Liu S, Zhang C (2010) Design and size optimization of compliant electrothermal microgripper. Chin Mech Eng 21(17):2028–2033

Zhang X, Lu Z, Gelinas D, Ciruna B, Sun Y (2011) Batch transfer of zebrafish embryos into multiwall plates. IEEE Trans Autom Sci Eng 8(3):625–632

Zhang Z, Yu Y, Liu X, Zhang X (2015a) A comparison model of V- and Z-shaped electrothermal microactuators. 2015 IEEE international conference on mechatronics and automation, August. Beijing, China, pp 2–5

Zhang Z, Yu Y, Liu X, Zhang X (2015b) Experimental study on the life and nonlinear actuation behaviors of V-shaped SU-8 electrothermal microactuators. 2018 IEEE 14th international conference on control and automation, June. Anchorage, AK, pp 12–15

Zhang Z, Yu Y, Zhang X (2017a) Vibration analysis of U-shaped beam electrothermal microactuators. 2017 2nd international conference on cybernetics, robotics and control, July 21–23. Chengdu, China, pp 80–84

Zhang Z, Yu Y, Liu X, Zhang X (2017b) Dynamic modelling and analysis of V- and Z-shaped electrothermal microactuators. Microsyst Technol 23(8):3775–3789

Zhang Z, Zhang W, Wu Q, Yu Y, Liu X, Zhang X (2017c) Closed-form modelling and design analysis of V- and Z-shaped electrothermal microactuators. Micromech Microeng 27:015023 (12 pp)

Zhang Z, Yu Y, Zhang X (2018a) Experimental testing and performance comparisons between V- and Z-shaped electrothermal microactuators. In: Proceedings of 2018 IEEE international conference on mechatronics and automation, August 5–8, Changchun

Zhang Z, Yu Y, Zhang X (2018b) Theoretical modal analysis and parameter study of Z-shaped electrothermal microactuators. Microsyst Technol 24(7):3149–3160

Zhang Z, Yu Y, Zhang X (2018c) Vibration modes and parameter analysis of V-shaped electrothermal microactuators. Shock Vib 2018:1080652 (12 pp)

Zhao Y, Sun H, Sha X, Gu L, Zhan Z, Li W (2019) A review of automated microinjection of zebrafish embryos. Micromachines 10(7):10010007(26 pp)

Zhou S, Chen P, Lu Z, Hoo N, Luo H, Ge R, Ong C, Lin W (2010) Speed optimization for micropipette motion during zebrafish embryo microinjection. In: 2010 11th international conference on control automation robotics & vision, Singapore, December 7–10